



Article

A Community Multi-Omics Approach towards the Assessment of Surface Water Quality in an Urban River System

David J. Beale ^{1,*}, Avinash V. Karpe ^{1,2}, Warish Ahmed ¹, Stephen Cook ³, Paul D. Morrison ⁴, Christopher Staley ⁵, Michael J. Sadowsky ⁵ and Enzo A. Palombo ²

¹ Land and Water, Commonwealth Scientific and Industrial Research Organization, P.O. Box 2583, Dutton Park, Queensland 4001, Australia; akarpe@swin.edu.au (A.V.K.); Warish.Ahmed@csiro.au (W.A.)

² Department of Chemistry and Biotechnology, Faculty of Science, Engineering and Technology, Swinburne University of Technology, P.O. Box 218, Hawthorn, Victoria 3122, Australia; epalombo@swin.edu.au

³ Land and Water, Commonwealth Scientific and Industrial Research Organization, Private Bag 10 Clayton South, Victoria 3169, Australia; Stephen.Cook@csiro.au

⁴ Australian Centre for Research on Separation Science, School of Applied Sciences, RMIT University, P.O. Box 2547, Melbourne, Victoria 3000, Australia; Paul.Morrison@rmit.edu.au

⁵ Biotechnology Institute, University of Minnesota, St. Paul, MI 55108, USA; cmstaley@umn.edu (C.S.); sadowsky@umn.edu (M.J.S.)

* Correspondence: David.Beale@csiro.au; Tel.: +61-7-3833-5774

Academic Editor: Susanne Charlesworth

Received: 19 January 2017; Accepted: 8 March 2017; Published: 14 March 2017

Abstract: A multi-omics approach was applied to an urban river system (the Brisbane River (BR), Queensland, Australia) in order to investigate surface water quality and characterize the bacterial population with respect to water contaminants. To do this, bacterial metagenomic amplicon-sequencing using Illumina next-generation sequencing (NGS) of the V5–V6 hypervariable regions of the 16S rRNA gene and untargeted community metabolomics using gas chromatography coupled with mass spectrometry (GC-MS) were utilized. The multi-omics data, in combination with fecal indicator bacteria (FIB) counts, trace metal concentrations (by inductively coupled plasma mass spectrometry (ICP-MS)) and in-situ water quality measurements collected from various locations along the BR were then used to assess the health of the river ecosystem. Sites sampled represented the transition from less affected (upstream) to polluted (downstream) environments along the BR. Chemometric analysis of the combined datasets indicated a clear separation between the sampled environments. *Burkholderiales* and *Cyanobacteria* were common key factors for differentiation of pristine waters. Increased sugar alcohol and short-chain fatty acid production was observed by *Actinomycetales* and *Rhodospirillaceae* that are known to form biofilms in urban polluted and brackish waters. Results from this study indicate that a multi-omics approach enables a deep understanding of the health of an aquatic ecosystem, providing insight into the bacterial diversity present and the metabolic output of the population when exposed to environmental contaminants.

Keywords: contaminated system; urban river system; metagenomics; metabolomics; trace metals; chemometrics

1. Introduction

Understanding the complex interaction between microbial communities and environmental changes, natural or anthropogenic, is a major research challenge [1]. Free-living microorganisms, such as planktonic bacteria in a water column or the diverse microbial community found in soils, would be

predicted to display large inter-individual metabolic variability as a result of their individual state, interaction with their surrounding environment and exposure to pollution sources. However, through a systems biology approach, harnessing the depth of knowledge provided by each microorganism can be aggregated and investigated in greater detail, and with increased throughput [2,3]. For example, microbial communities are known to colonize most environments, including contaminated sites or harsh climatic environments [4–6]. These communities have been demonstrated to metabolize recalcitrant contaminants (via bioremediation) and have been observed to thrive under extreme conditions [7]. The recent development of omics-based techniques has enabled environmental microbiologists to recognize and characterize such microbial communities as an imperative ecological parameter in monitoring polluted and extreme environments, either by detecting community shifts in response to contaminant(s) or their resilience towards climatic or physico-chemical disturbances [7]. In this context, the application of metagenomics and meta-transcriptomics has been vital in detailing the microbial community present and its potential activity, and techniques such as meta-proteomics and metabolomics have provided insight into the specific proteins and metabolites that are expressed [2].

Desai et al. [7], amongst others, proposed that the simultaneous analyses of multiple omics-based approaches would lead to a system-wide assessment of site-specific microorganisms and their underlying physico-chemical disturbances; they focused on characterizing the protein synthesis and carbon and carbohydrate metabolism of the sampled population at xenobiotic/anthropogen contaminated sites. To an extent, many researchers have already started employing multi omics-based techniques to their research. Bullock et al. [8] investigated the microbial activity in relation to organic matter degradation and turnover at various locations in the Mid-Atlantic Bight. Date et al. [9] used metagenomics and ^{13}C labelled metabolomics to monitor the metabolic dynamics of fecal microbiota. Hook et al. [10] investigated contaminated sediments using transcriptomics and metabolomics in order to better understand the modes of toxic action within contaminated ecosystems. Specifically, the function of transcripts with altered abundance of *Melita plumulosa* (an epibenthic amphipod) was investigated following whole-sediment exposure to a series of common environmental contaminants. Such contaminants included pore-water ammonia, bifenthrin and fipronil (pesticides), diesel and crude oil (petroleum products), and metals (Cu, Ni, and Zn). Subsequent data integration and hierarchical cluster analysis demonstrated grouped transcriptome and metabolome expression profiles that correlated with each specific contaminant class. Many of the transcriptional changes observed were consistent with patterns previously described in other crustaceans [11]. Likewise, Hultman et al. [5] undertook a similar study investigating the microbial metabolism of permafrost. They used several omics approaches, combined with post-data analysis, to determine the phylogenetic composition of microbial communities of intact permafrost, the seasonally thawed active layer and thermokarst bog (surfaces of marshy hollows). The multi-omics strategy revealed good correlation of process rates for methanogenesis (the dominant process), in addition to providing insights into novel survival strategies for potentially active microbes in permafrost [5].

The inclusion of metabolomics in (meta)transcriptomics and metagenomics investigations has enabled researchers to assess biochemical profile variations of entire microbial communities living in contaminated sites [6,12]. Metabolomics is a well-established scientific field that focuses on the study of low molecular weight metabolites (typically <1000 Da) within a cell, tissue or bio-fluid [13–15]. Furthermore, the application of environmental metabolomics is an expanding field within the metabolomics platform. Environmental metabolomics assesses and characterizes the interactions of living organisms within their environment [4] and is traditionally used as a tool to investigate environmental factors, either physical or chemical, and their impact to a specific organism. For example, Gómez-Canela et al. [16] used targeted environmental metabolomics to investigate *Gammarus pulex* (a freshwater amphipod crustacean) following controlled exposures to selected pharmaceuticals in water. Similarly, Cao et al. [17] studied the bioaccumulation and metabolomics responses in *Crassostrea hongkongensis* (an oyster) impacted by different levels of metal pollution; and Ji et al. [18] studied the impact of metal pollution on *Crangon affinis* (a shrimp). In addition, community

metabolomics extends the application of environmental metabolomics even further through the investigation of all metabolites expressed from an entire microbial community, thus enabling a meta-metabolomics approach [6].

The advancement of omics-based techniques and their integration (coined multi-omics) have contributed towards the fields of environmental and molecular biology, thereby pushing the boundaries of our understanding of microbial physiology [19]. To date, such studies have focused on specific pollution events (e.g., the Deepwater Horizon oil spill [20]), the assessment of biotechnology/bioremediation (e.g., bioremediation of steroids in the environment [21]) or used to characterize well-controlled engineered systems (e.g., anaerobic bioreactors [22,23]). To the best of our knowledge, such an approach has not been used to characterize a system as part of a water quality monitoring survey. The application of metagenomics or metabolomics in isolation has been applied with some success [24]. For example, metagenomics has been applied to assess drinking water microbial populations after various treatment methods [25] and assess river microbiomes across various land use types [26]. Beale et al. [27] used metabolomics with physico-chemical data to assess water pipeline infrastructure and water pipe biofilms, characterizing biofilms based on pipe material and the excreted metabolites that pass from the biofilm into the water stream. A similar study was used to investigate impacts of exposure to chemicals of emerging concern relative to other stressors in fathead minnows, which was used as a model species [28].

The current study herein merges bacterial metagenomics and community metabolomics with additional physico-chemical data, thus using a multi-omics based approach to investigate an urban river system. It is anticipated that such an approach would provide an additional layer of information on top of traditional water quality monitoring parameters that will ultimately result in a deeper understanding of the diverse microbial population present, enabling researchers to characterize environmental systems, not based on inferred water quality data but as an interconnected complex system. Furthermore, it is anticipated that a multi-omics approach will enable a better appreciation of the system's resilience to urban physical and/or chemical changes and stress.

2. Materials and Methods

2.1. Water Sampling

Water samples were collected from five sites along the Brisbane River (BR), Queensland (Qld), Australia during the low outgoing tide in December 2013. For reference, the BR sampling sites are presented in Figure 1, are annotated with stars and designated BR₁ to BR₅. Triplicate samples were collected from each site at one sampling event, giving a total of 15 water samples. The in-situ measurements of temperature (°C), conductivity (mS/cm), pH, salinity (ppt), turbidity (NTU), and dissolved oxygen (mg·L⁻¹) were made at the time of collection using a calibrated AQUAprobe AP-300 water quality probe (Aquaread, Broadstairs, Kent, UK). Moreover, each site was matched, by location and date, with sample sites from the Healthy Waterways "Ecosystem Health Monitoring Program (EHMP)" water quality monitoring program [29]. Of note, Healthy Waterways is a not-for-profit, non-government, membership-based organization working to protect and improve waterway health in South East Qld. Data from the EHMP matched sites were included in the analysis in order to expand the breadth of physico-chemical data collected.

At each site, triplicates of 10-liter water samples were collected from 30 cm below the water surface in sterile carboy containers. The water samples were then transported on ice to the laboratory, and processed within 6–8 h. Sample site characteristics and GPS coordinates are provided in Table 1. In addition, complementary data from the matched EHMP sites are provided in Table 2. Furthermore, site BR₁ is located on the upper reaches of the BR. This site receives overflow of water from the Wivenhoe Reservoir. Site BR₂ is located in a peri-urban non-sewered catchment. Site BR₃ is at a major tributary of the Brisbane River. The catchment where site BR₃ is located has residential and industrial developments and is serviced by a wastewater treatment plant (WWTP). Sites BR₅ and BR₆ are located

on the lower reaches of the river, in highly urbanized areas and is tidally influenced. The catchment had not received any rainfall 7 days prior to sampling.

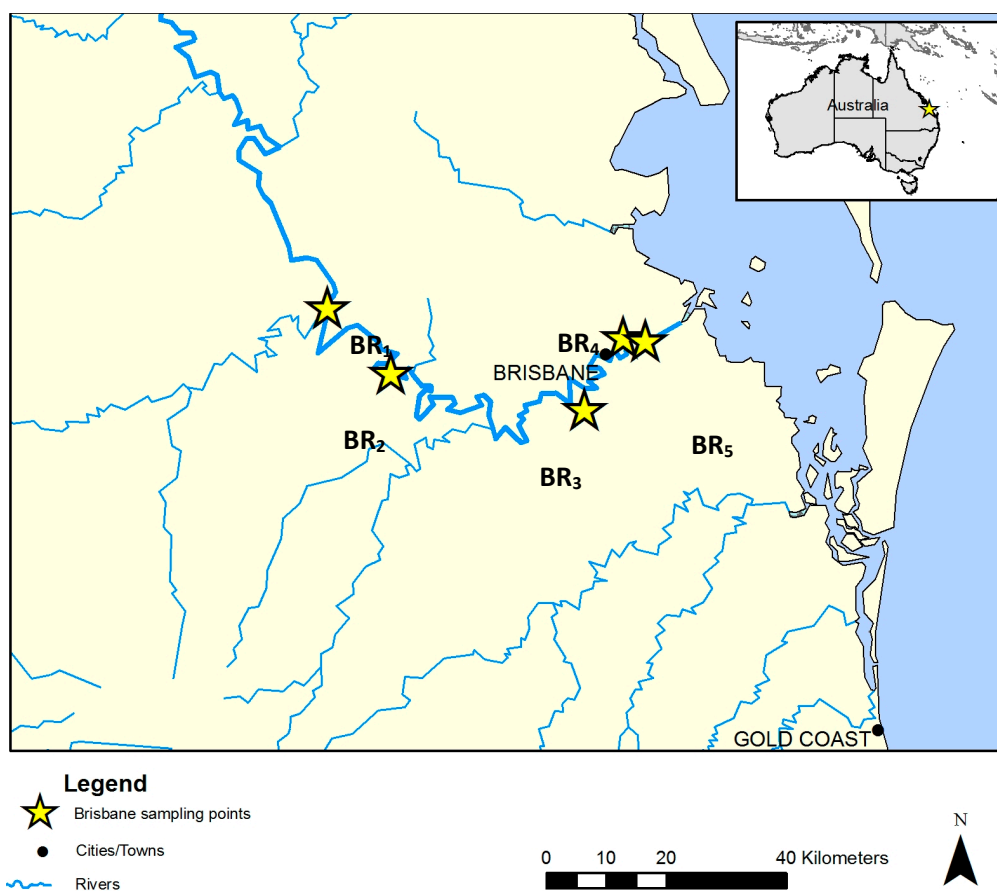


Figure 1. Map of the Brisbane River (BR) and the selected sampling sites (BR₁–BR₅).

2.2. Water Quality Analysis

2.2.1. Dissolved Organic Carbon

Samples were filtered through a 0.45 µm pore size (47 mm diameter) hydrophilic membrane (Durapore polyvinylidene difluoride, PVDF, Millipore, Tokyo, Japan), and the dissolved organic carbon in 30 mL of sample was determined in triplicate using a 820 TOC (total organic carbon) analyzer (Model: Sievers, GE Analytical Instruments Inc., Boulder, CO, USA).

2.2.2. Trace Metals

A 10 mL aliquot of water from each site was filtered through a 0.45 µm pore size nitrocellulose membrane (Millipore) prior to acidifying to 2% with concentrated nitric acid (AR grade; Sigma Aldrich, Castle Hill, NSW, Australia). Each sample was prepared in triplicate, with three samples collected per site ($n = 45$, for all five EHMP sites). Aluminum (Al), cadmium (Cd), cobalt (Co), chromium (Cr), copper (Cu), iron (Fe), lead (Pb), nickel (Ni) and zinc (Zn) were determined using an Agilent 7700x quadrupole-type ICP-MS (Agilent Technologies, Mulgrave, VIC, Australia) equipped with an Agilent ASX-520 auto sampler. The instrument was operated in He-mode. The integration time was 0.3 s per mass, 1 point per mass, 3 replicates and 100 sweeps per replicate. All samples and standards were stored in Falcon tubes (15 mL) that were rinsed with 2% nitric acid, and kept at 4 °C until analyzed. All consumables were soaked in 10% nitric acid for at least 24 h and rinsed repeatedly with MilliQ and 2% nitric acid (in MilliQ water) before use.

Table 1. Sample site description and in-situ water quality characteristics. Water quality parameters were analyzed in triplicate ($n = 3$) and the relative standard deviation as a percentage (%RSD) are presented in the parentheses.

BR Site	EHMP Site	GPS Coordinates	Temp. (°C)	Conductivity (mS·cm ⁻¹)	Salinity (ppt)	pH	Turbidity (NTU)	DOC * (mg·L ⁻¹)	Site Characteristics	Suspected Source of Pollution
BR ₁	714	27°23'58" S; 152°36'26" E	21.7 (0.4)	0.39 (<0.1)	0.19 (<0.1)	7.14 (<0.1)	0.5 (1.7)	9.32 (0.8)	Rural	Wildlife, waterfowl, recreational activities.
BR ₂	711	27°29'51" S; 152°42'7" E	28.1 (<0.1)	0.53 (<0.1)	0.25 (<0.1)	8.00 (<0.1)	5.2 (0.1)	9.30 (0.4)	Rural	Cattle, horses, septic tanks, wildlife.
BR ₃	718	27°33'8" S; 152°59'31" E	26.6 (<0.1)	0.7 (<0.1)	0.32 (<0.1)	7.00 (<0.1)	137 (0.2)	8.88 (0.5)	Peri urban, tidally influenced	Wastewater treatment plants, waterfowls.
BR ₄	703	27°26'38" S; 153°3'3" E	25.7 (<0.1)	46.5 (<0.1)	30.17 (<0.1)	7.77 (<0.1)	15.3 (4.4)	4.35 (0.5)	Urban	Recreational activities, tidal influence.
BR ₅	702	27°26'56" S; 153°5'0" E	25.4 (<0.1)	46.9 (<0.13)	30.47 (0.3)	7.71 (<0.1)	11.6 (0.1)	5.02 (1.2)	Urban	Port, industrial activities, tidal influence.

Note: EHMP is defined as "Ecosystem Health Monitoring Program". * DOC is defined as dissolved organic carbon.

Table 2. Sample site description and EHMP site matched water quality characteristics.

BR Site	EHMP Site	Chlorophyll a (µg·L ⁻¹)	Light Penetration (Secchi Depth, m)	Phosphorus as P		Nitrogen as N			
				FRP * (µg·L ⁻¹)	Total (µg·L ⁻¹)	Ammonia (µg·L ⁻¹)	Organic (µg·L ⁻¹)	Oxides (µg·L ⁻¹)	Total (µg·L ⁻¹)
BR ₁	714	6.30	0.45	31	61	<4	323	13	340
BR ₂	711	0.37	0.15	240	320	12	368	500	880
BR ₃	718	1.50	0.60	260	270	6	254	550	810
BR ₄	703	2.24	0.50	93	140	8	202	210	420
BR ₅	702	2.13	0.85	64	79	10	190	100	300

Note: EHMP is defined as "Ecosystem Health Monitoring Program". * FRP is defined as filterable reactive phosphorus.

2.2.3. Enumeration of Fecal Indicator Bacteria (FIB)

The membrane filtration method was used for the isolation and enumeration of FIB. Serial dilutions of water samples were made in sterile MilliQ water, and filtered through 0.45- μm pore size nitrocellulose membrane (Merck Millipore, Bayswater, VIC, Australia). Dilutions were placed on modified membrane-thermotolerant *Escherichia coli* agar medium (modified mTEC agar, Difco, Detroit, MI, USA) and membrane-*Enterococcus* indoxyl-D-glucoside (mEI) agar (Difco) for the isolation of *E. coli* and *Enterococcus* spp., respectively. Modified mTEC agar plates were incubated at 35 °C for 2 h to recover stressed cells, followed by incubation at 44 °C for 22 h, while the mEI agar plates were incubated at 41 °C for 48 h [30,31].

2.3. Biomass Collection from Water Samples

Four sub-samples (2 L) of the 10 L parent sample were filtered through 0.45 μm pore size nitrocellulose membrane. Multiple membranes were used in case of membrane clogging due to sample particulates. The membrane(s) were immediately transferred into a sterile 15 mL Falcon tube containing phosphate buffered saline (Sigma-Aldrich, St. Louis, MO, USA). The sample tube was vortexed for 5 min to detach the microbial biomass from the membrane, followed by centrifugation at 4500 g for 15 min at 4 °C to obtain a pellet [32]. One sample tube was used for DNA extraction and subsequent metagenomics analysis. The remaining three tubes were used for metabolite extraction and subsequent community metabolomic analysis.

2.4. Metagenomic Analysis

2.4.1. DNA Extraction

DNA was extracted from the pellet obtained from each water sample using the MO BIO PowerSoil[®] DNA Isolation Kit (MO BIO Laboratories, Carlsbad, CA, USA) as per Ahmed et al. [33]. The extracted DNA samples were quantified using a ND-1000 spectrophotometer (NanoDrop Technology, Wilmington, DE, USA).

2.4.2. PCR and Illumina MiSeq Sequencing

The V5 and V6 regions of the 16S rRNA gene were amplified using the primer set described previously [34]. Noting that the V5 and V6 region has been shown to provide equivalent diversity estimates to the V4 region, and is similar to full length 16S rRNA sequencing [35]. Amplicons from each sample were pooled in equal amounts. All samples were paired-end sequenced at a length of 300 nucleotides [nt] in each direction by the University of Minnesota Genomic Center (Minneapolis, MN, USA), using version 3 chemistry on the MiSeq platform. Raw data were deposited in the NCBI Sequence Read Archive under BioProject accession number SRP062949.

2.4.3. Sequence Data Analysis

Sequence processing was performed using mothur software ver. 1.33.3 (<http://www.mothur.org>) [36]. Sequences were first trimmed to 150 nt and paired-end joined using fastq-join [37]. Quality trimming was performed to remove sequences with average quality scores <35 over a window of 50 nt, homo-polymers >8 nt, ambiguous bases, or mismatches to primer sequences. High-quality sequences were aligned against the SILVA database ver. 115 [38]. Sequences were further quality trimmed using a 2% pre-cluster [39,40], and chimera removal using UCHIME [41]. Assignment of OTUs was performed at 97% identity using the furthest-neighbor algorithm. Taxonomic assignments were made against the Ribosomal Database Project database ver. 9 [42]. For comparisons among BR sampling sites, sequence reads for each replicate were rarefied by random subsample to 25,000 (75,000 sequence reads per site).

2.5. Community Metabolomics Analysis

Overall, 45 samples were collected from five sample sites. Of note, each sample site was collected in triplicate and then subsequently analyzed in triplicate. All samples were derivatized prior to analyses by gas chromatography-mass spectrometry (GC-MS) as mentioned in previous studies [43–45]. Briefly, a 1.0 mL aliquot of ice cold methanol (LC grade, ScharLab, Sentemanat, Spain) and MilliQ water (50:50 *v/v*) were added to each sample pellet, then vortexed briefly before centrifugation at 572.5 g for 15 minutes at 4 °C. Adonitol (20.0 µg/mL, HPLC grade, Sigma-Aldrich, Castle Hill, NSW, Australia) was added as an internal standard. A 100.0 µL aliquot of the supernatant was then transferred to a fresh tube and dried in a centrifugal evaporator at 210 g and 37 °C (Model number: RVC 2-18; Martin Christ Gefriertrocknungsanlagen GmbH, Osterode, Germany).

2.5.1. Sample Silyl Derivatization

For GC-MS analysis, dried samples were derivatized using 40.0 µL methoxyamine HCl (20 mg/mL in pyridine) followed by 70.0 µL *N,O*-bis(trimethylsilyl)trifluoroacetamide (BSTFA) in 1% trimethylchlorosilane (TMCS). Samples were then briefly vortexed before being transferred to GC-MS vials and microwaved for 3 min at 120 °C/600 W using a Multiwave 3000 system (Perkin Elmer Inc., Melbourne, VIC, Australia).

2.5.2. Single Quadrupole GC-MS

Single quadrupole GC-MS was performed as previously reported [46,47]. Briefly, an Agilent 7890B gas chromatograph (GC) oven coupled to a 5977A mass spectrometer (MS) detector (Agilent Technologies) was used. The GC-MS system was fitted with a 30 m HP-5MS column, 0.25 mm internal diameter and 0.25 µm film thickness. Injections (1.0 µL) were performed in 1:10 split mode, with the oven held at an initial temperature of 70 °C for 2.0 min. The temperature was then ramped-up to 300 °C at 7.5 °C·min⁻¹ and the final temperature (300 °C) was held for 5.0 min. The transfer line was held at 280 °C. Total ion chromatogram (TIC) mass spectra were acquired within a range of 45–550 *m/z*, with a 2.89 spectra·s⁻¹ acquisition frequency. A solvent delay time of 7.5 min ensured that the source filament was not saturated or damaged. Data acquisition and spectral analysis were performed using the Qualitative Analysis software (Version B.07.00) of MassHunter workstation. Qualitative identification of the compounds was performed according to the Metabolomics Standard Initiative (MSI) chemical analysis workgroup [48] using standard GC-MS reference metabolite libraries (NIST 14, Fiehn and Golm) and with the use of Kovats retention indices based on a reference *n*-alkane standard (C8–C40 Alkanes Calibration Standard, Sigma-Aldrich, Castle Hill, NSW, Australia). For peak integration, a 5-point detection filtering (default settings) was set with a start threshold of 0.2 and stop threshold of 0.0 for 10 scans per sample.

2.6. Data Integration and Statistical Analysis

The metagenomics, metabolomics, trace metal and water quality data were subjected to further statistical analysis involving multivariate analyses of Principal Component Analysis (PCA) and Partial Least Square-Discriminant Analysis (PLS-DA) using SIMCA 14.1 (MKS Data Analytics Solutions, Uméa, Sweden). For the merging of these multiple datasets, the data was first imported, matched by sample location identifiers and log transformed. The analyses provided spatial distribution of various bacteria, their intracellular and extracellular metabolic activity and the relationships between the water quality parameters investigated.

3. Results

3.1. Physico-Chemical Data

Analysis of the physico-chemical parameters measured during sampling and the data available on the EHMP website revealed the level of degradation of the sampled system as a temporal snapshot.

The salinity measurements of the sites indicate that BR₄ and BR₅ are above the recommended threshold for a freshwater ecosystem in the “Australian and New Zealand Guidelines for Fresh and Marine Water Quality (AWA)” [49] (threshold value of ca. 1.1 ppt). However, it is noteworthy to mention that these sites are influenced by the tide and the nearby estuary, although samples were collected during low tide. All the other sites were within the acceptable threshold for salinity (Table 1).

The AWA guidelines also state that lowland river systems have turbidity limits between 6–50 NTU. For the sites sampled, BR₃ was observed to be above this threshold (137 NTU); the tidal influenced sites (BR₄ and BR₅) were also within this range but are considered high for estuaries/marine environments (which have a threshold of 0.5–10 NTU).

All sites were within the acceptable range stated in the guidelines with respect to pH (6.5–8.0). However, site BR₂ was observed at the maximum range of the threshold (pH 8.0). For the EHMP derived data, chlorophyll a levels ($5 \mu\text{g}\cdot\text{L}^{-1}$) were observed to be within acceptable limits with the exception of site BR₁ ($6.3 \mu\text{g}\cdot\text{L}^{-1}$). The total phosphorous (TP) (acceptable level $\leq 50 \mu\text{g}\cdot\text{L}^{-1}$) was high for all the sites (above $50 \mu\text{g}\cdot\text{L}^{-1}$), with sites BR₂ ($320 \mu\text{g}\cdot\text{L}^{-1}$), BR₃ ($270 \mu\text{g}\cdot\text{L}^{-1}$), and BR₄ ($140 \mu\text{g}\cdot\text{L}^{-1}$) observed to contain exceptionally high TP when compared to the threshold value. Likewise for filterable reactive phosphate (FRP) (acceptable level $\leq 20 \mu\text{g}\cdot\text{L}^{-1}$), all sites were observed above the guideline value, with sites BR₂ ($240 \mu\text{g}\cdot\text{L}^{-1}$) and BR₃ ($260 \mu\text{g}\cdot\text{L}^{-1}$) the highest. For total nitrogen (TN) (acceptable levels $\leq 500 \mu\text{g}\cdot\text{L}^{-1}$), sites BR₂ ($880 \mu\text{g}\cdot\text{L}^{-1}$) and BR₃ ($810 \mu\text{g}\cdot\text{L}^{-1}$) were above the guideline value. Nitrogen oxide(s) (NO_x) (acceptable level $\leq 60 \mu\text{g}\cdot\text{L}^{-1}$) was high for all sites with the exception of BR₁ ($31 \mu\text{g}\cdot\text{L}^{-1}$). Sites BR₂ ($500 \mu\text{g}\cdot\text{L}^{-1}$), BR₃ ($550 \mu\text{g}\cdot\text{L}^{-1}$), BR₄ ($210 \mu\text{g}\cdot\text{L}^{-1}$) and BR₅ ($100 \mu\text{g}\cdot\text{L}^{-1}$) were observed to have significantly higher NO_x content than the threshold. Lastly, all sites were below the threshold regulatory limit for ammonium based nitrogen (NH₄⁺) ($<20 \mu\text{g}\cdot\text{L}^{-1}$).

3.2. Trace Metals

Heavy metal pollution of waterways is typically associated with mining activities or discharges from manufacturing industries. Heavy metal pollution in water and sediments can have serious effects on the aquatic ecosystem and can make water unsuitable for livestock and/or human consumption. Furthermore, some animals (i.e., fish, shellfish and oysters) can also “bio-accumulate” metals [17], making them unsafe for consumption. As such, the concentration of metals in an urban stream is of interest, more so when the stream has the potential to further impact downstream fisheries in estuaries and marine environments.

In the context of this study, soluble metals in the sampled river were analyzed because they would most likely impact the planktonic biota (in terms of abundance and diversification) and their metabolism (i.e., metabolic output). However, metals bound within sediments and biofilms, although important, were considered outside the scope of this investigation and is the focus of future work.

All trace metals analyzed were below the trigger values set for freshwater aquatic ecosystems at the 90% level of protection of species in the guidelines. The trigger values were set at $80 \mu\text{g}\cdot\text{L}^{-1}$ for aluminum, $0.4 \mu\text{g}\cdot\text{L}^{-1}$ for cadmium, $1.8 \mu\text{g}\cdot\text{L}^{-1}$ for copper, $5.6 \mu\text{g}\cdot\text{L}^{-1}$ for lead, $13 \mu\text{g}\cdot\text{L}^{-1}$ for nickel, and $15 \mu\text{g}\cdot\text{L}^{-1}$ for zinc. The guidelines have no set limit for chromium, cobalt and iron [49]. However, as indicated in Table 3, site BR₃ was observed to have elevated levels for all the metals analyzed. In particular, site BR₃ was observed to have significantly higher concentrations of aluminum ($2.01 \mu\text{g}\cdot\text{L}^{-1}$) and iron ($4.53 \mu\text{g}\cdot\text{L}^{-1}$) compared to the up-stream and down-stream sampling sites. It also was observed to have slightly higher concentrations of cobalt ($2.38 \text{ng}\cdot\text{L}^{-1}$), chromium ($1.0 \text{ng}\cdot\text{L}^{-1}$), copper ($8.1 \text{ng}\cdot\text{L}^{-1}$), lead ($7.6 \text{ng}\cdot\text{L}^{-1}$) and nickel ($36.9 \text{ng}\cdot\text{L}^{-1}$). It is noteworthy to mention that site BR₃ was located near a wastewater treatment plant and is located at the junction of a side stream that enters into the BR.

Table 3. Concentrations of metals in the water sourced from different sites and attributed to different sources. Values in the parenthesis denote standard deviations between the samples ($n = 9$).

BR Site	Concentration of Metals (RSD %)								
	Aluminum (Al, ng·L ⁻¹)	Cadmium (Cd, ng·L ⁻¹)	Cobalt (Co, ng·L ⁻¹)	Chromium (Cr, ng·L ⁻¹)	Copper (Cu, ng·L ⁻¹)	Iron (Fe, ng·L ⁻¹)	Lead (Pb, ng·L ⁻¹)	Nickel (Ni, ng·L ⁻¹)	Zinc (Zn, ng·L ⁻¹)
BR ₁	1.0 (>0.1)	<0.04	0.04 (4.7)	<0.02	3.0 (0.1)	<0.571	<0.06	<0.06	4.6 (2.3)
BR ₂	1.0 (>0.1)	<0.04	0.14 (5.3)	<0.02	3.1 (0.1)	32.0 (3.0)	<0.06	0.2 (0.1)	3.6 (0.6)
BR ₃	2008 (4.9)	<0.04	2.38 (2.4)	1.0 (0.1)	8.1 (0.1)	4529.7 (188.1)	7.6 (0.2)	2.8 (0.1)	36.9 (1.2)
BR ₄	1.0 (>0.1)	<0.04	0.15 (10.1)	<0.02	4.3 (0.6)	94.1 (59.3)	<0.06	0.4 (0.2)	6.2 (3.1)
BR ₅	11.0 (1.9)	<0.04	0.26 (3.4)	<0.02	4.0 (0.2)	234.7 (27.6)	<0.06	0.4 (0.1)	6.8 (1.5)

Table 4. Microbial water quality based on the various coliform counting methods. Values in the parenthesis indicate standard deviations ($n = 9$).

BR Site	Fecal Indicator Bacteria (FIB) ^a		Recreational Microbial Water Quality Assessment ^b			Microbial Water Quality Assessment Category (MAC)
	<i>E. coli</i> /100 mL Geometric Mean (Std. Dev.)	<i>Enterococcus spp.</i> /100 mL Geometric Mean (Std. Dev.)	<i>Enterococcus spp.</i> (<33 CFU/100 mL (%))	<i>Enterococcus spp.</i> (>157 CFU/100 mL (%))	Standardized (95th Percentile ^c)	
BR ₁	15 (4)	4 (2)	100	0	2	A
BR ₂	69 (18)	22 (5)	100	0	2	A
BR ₃	307 (49)	544 (85)	0	100	13,300	D
BR ₄	149 (25)	189 (24)	0	89	12,900	D
BR ₅	88 (16)	163 (37)	0	56	10,600	D

^a Determined using the geometric mean of nine samples ($n = 9$); ^b Recreational Microbial Water Quality Assessment calculated using *Enterococcus spp.* data following the NH&MRC "Guidelines for Managing Risks in Recreational Water"; ^c Calculated using the ranked method ($n = 9$).

3.3. Fecal Indicator Bacteria (FIB)

Among the 15 water samples analyzed from the five sites, all samples yielded culturable *E. coli* and *Enterococcus* spp. The concentrations of *E. coli* and *Enterococcus* spp. in water samples ranged from 15–307 colony forming units (CFU) and 4–544 CFU per 100 mL of water, respectively (Table 4).

The concentrations of *E. coli* and *Enterococcus* spp. were much greater in water samples from sites BR₃ and BR₄ compared to the other sites. Furthermore, sites BR₃, BR₄ and BR₅ were all classed as poor quality (Class D) using the Microbial Water Quality Assessment Category (MAC) framework outlined in the Australian recreational water guidelines. It should be noted that sites BR₁, BR₂, and BR₃ all had evidence of wildlife within the sampling sites. Sites BR₄ and BR₅ are also known human recreational locations and may have wildlife present that was not observed at the time of sampling. These wildlife factors may influence the FIB measurements obtained [50,51]. Interestingly, in a parallel investigation by Ahmed et al. [33], it was observed that human fecal contamination was present at site BR₃ using a microbial source tracking toolbox (MST) approach targeting human-wastewater-associated *Bacteroides* HF183 molecular markers [33]. In addition, Aves (avian) fecal contamination was observed using the avian-associated GFD molecular marker at sites BR₁, BR₃, BR₄, and BR₅; Bovinae (cow) fecal contamination was observed using the cattle-associated CowM3 molecular marker at site BR₂ and *Equidae* (horse) fecal contamination was observed using a horse-associated molecular marker at site BR₄.

3.4. Metagenomics

The estimated Good's coverage of the sample groups (75,000 sequence reads per site, with 3 independent samples subsampled to 25,000 sequence reads) ranged from 97% to 100%, with an average of 96% ± 1.2% among all samples. An average Shannon diversity index of 5.00 ± 0.24, OTU richness value of 1725 ± 172, and abundance-based coverage estimate of 4024 ± 1035 richness were observed among all samples. Table 5 provides a summary of the bacterial metagenomics data based on observed and unique features per order, family and genera for each sampled site. Figure 2 illustrates the bacterial order profile summary of the sampled sites and Figure 3 provides an overview of the site features in terms of similarity and uniqueness as presented as a Venn diagram.

Table 5. Summary of site bacterial metagenomics characterization.

BR Sites	Features per Group			Unique Features per Site		
	Order	Family	Genus	Order	Family	Genus
BR ₁	121	226	592	3	5	54
BR ₂	118	223	562	0	2	33
BR ₃	102	186	389	1	4	20
BR ₄	117	238	667	3	11	70
BR ₅	116	248	741	4	13	78

The unique Family features for the sites were *Clostridiales incertae sedis*, *Desulfonatronaceae*, *Corynebacteriaceae*, *GpX*, and *Dermatophilaceae* for Site BR₁; *Incertae Sedis*, *Aquificaceae* for site BR₂; *Ktedonobacteraceae*, *Herpetosiphonaceae*, *Aerococcaceae*, and *Spirochaetales incertae sedis* for site BR₃, *Brevinemataceae*, *Euzebyaceae*, *Dietziaceae*, *Thermoactinomycetaceae* 1, *Saccharospirillaceae*, *Cohaesibacteraceae*, *Dermacoccaceae*, *Clostridiaceae* 2, *Psychromonadaceae*, *Rubrobacteraceae*, and *Thiohalorhabdus* for site BR₄; and, *Aquificales incertae sedis*, *Thermosporotrichaceae*, *Desulfarculaceae*, *Congregibacter*, *Cellulomonadaceae*, *Acholeplasmataceae*, *Bartonellaceae*, *Thermolithobacteraceae*, *Lactobacillaceae*, *Leuconostocaceae*, *Micromonosporaceae*, *Promicromonosporaceae*, and *Sphaerobacteraceae* for site BR₅.

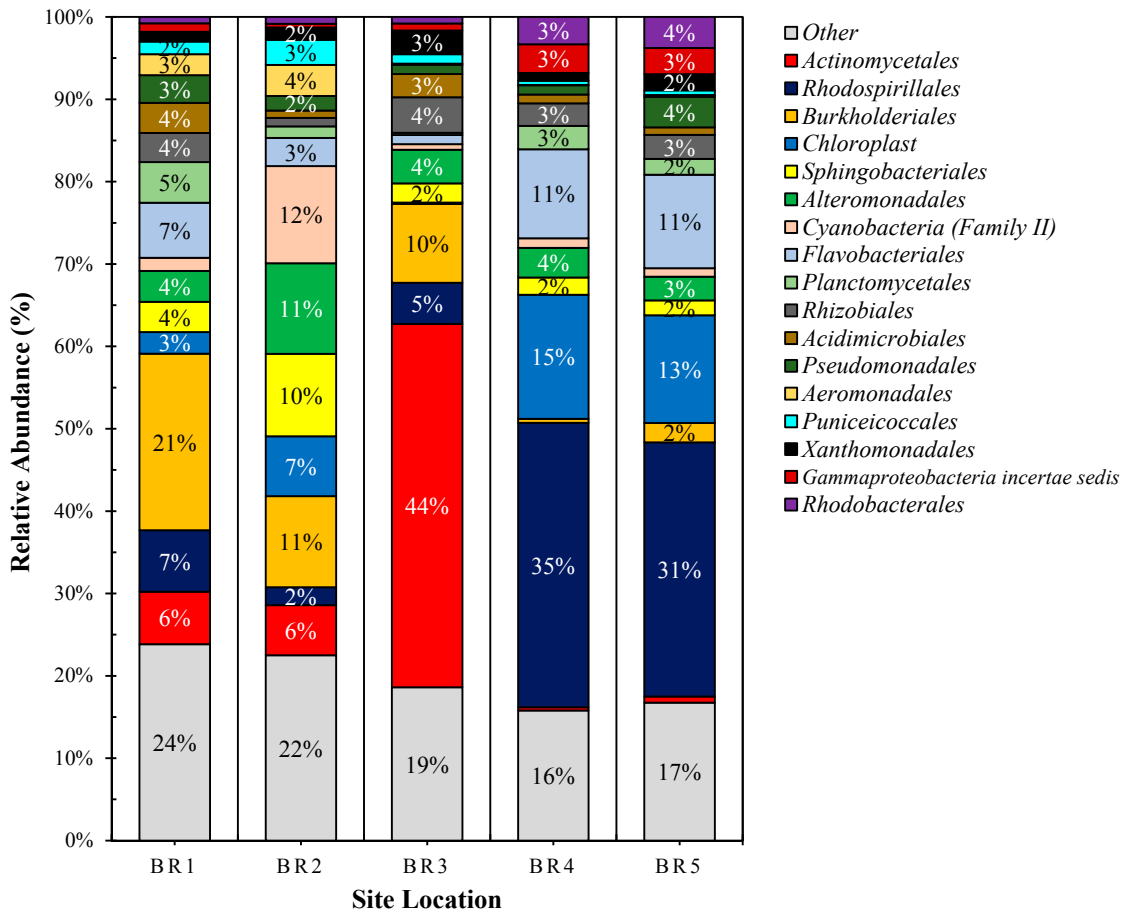


Figure 2. Bacterial order (top 17) profile of the BR sample sites. Note: ‘others’ represent orders less than 2% of the total sequence abundance.

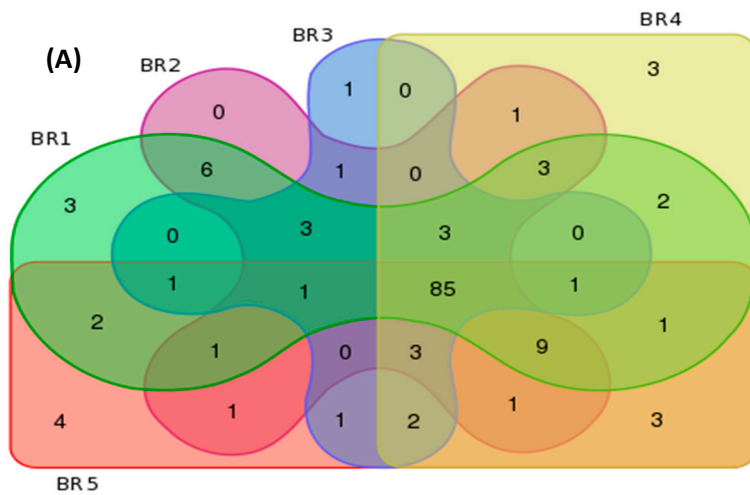


Figure 3. Cont.

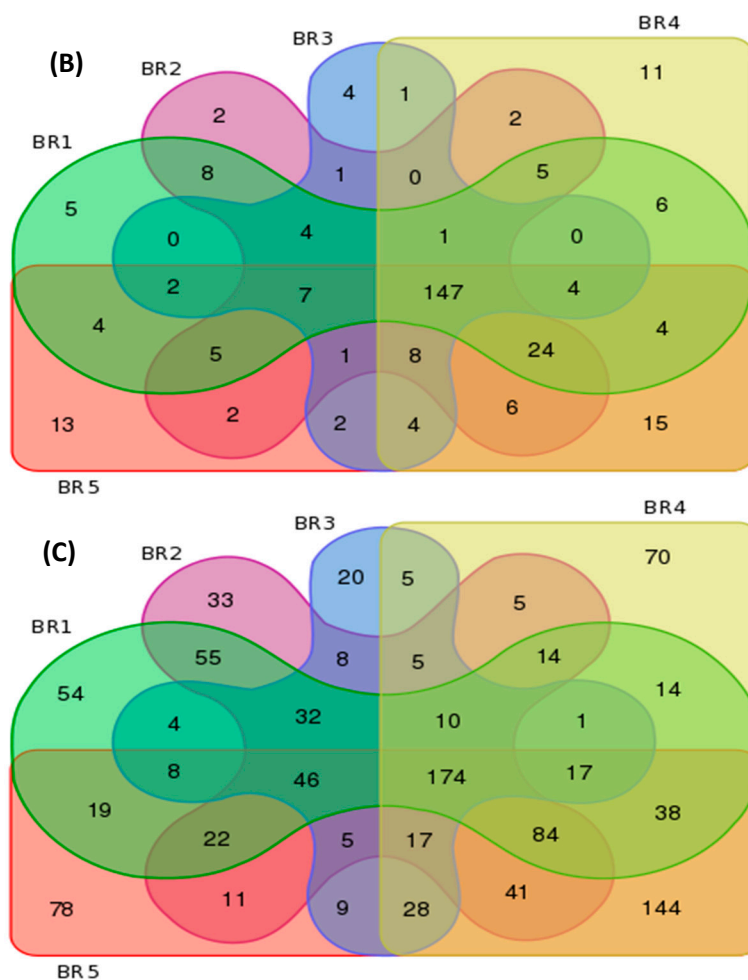


Figure 3. Bacterial metagenomics similarity and uniqueness characterization based on (A) order; (B) family and (C) genus.

3.5. Community Metabolomics

The GC-MS analysis of the samples indicated a presence of 289 peaks per chromatogram, of which 54 were considered statistically significant (S/N ratio ≥ 50 with an adjusted p -value ≤ 0.05). Univariate and multivariate statistical tools such as t -test, Principal Component Analysis (PCA) and Partial Least Square-Discriminant Analysis (PLS-DA) were used to analyze the distribution and classification of the various metabolites. Due to the unsupervised nature of the data and the number of sample sites, PCA was observed as a less satisfactory method to discriminate between the metabolite distributions. As such, samples were processed further using Partial Least Square-Discriminant Analysis (PLS-DA). PLS-DA is used to examine large datasets and has the ability to measure linear/polynomial correlation between variable matrices by lowering the dimensions of the predictive model, allowing easy distribution between the samples and the metabolite features that cause the distribution.

The data quality of PLS-DA model was assessed by the linearity (R^2X) and predictability (Q^2), which were observed at 0.8294 and 0.565, respectively. These are indicative of a model that reasonably fits the data and has a weak/moderate predictive capability (~ 0.5). Figure 4A illustrates the PLS-DA score scatter plot of the metabolomic dataset groups (sample sites), and Figure 4B illustrates the loading scatter plot of the observed metabolites. The majority of the identified metabolites were sugars, fatty acids and amino acids. Secondary metabolites such as perillyl alcohol, lithocholic acid and phytol were also observed. As biological datasets tend to significantly vary from sample to sample, a distance of observation (DModX) analysis was also used to identify and eliminate

any outliers. DModX is the normalised observational distance between variable set and X modal plane and is proportional to variable's residual standard deviation (RSD). "DCrit (critical value of DModX)", derived from the F-distribution, calculates the size of observational area under analysis. The DModX plot (not shown) data indicate that no samples exceeded the threshold for rejecting a sample. The threshold for a moderate outlier is considered when the sample DModX value is twice the DCrit at 0.05, which, in this instance, was 2.897 (DCrit = 1.435). Table 6 lists the 'identified' significant metabolites after Benjamini-Hochberg adjustment. The unique metabolite features for the sites were Unknown Compound 13 (MW = 218.2) for site BR₂; Xylitol (dTMS), L-Arabinose (4TMS), Unknown Compound 4 (MW = 325.2), and Unknown Compound 15 (MW = 189.1) for site BR₃; Phytol mixture of isomers, Erythritol (4TMS) and D-Fructose (5TMS) for site BR₄; and, Unknown Compound 18 (MW = 278.2) and Unknown Compound 9 (MW = 325.2) for site BR₅. Figure 5 provides an overview of the site metabolite features in terms of similarity and uniqueness as presented as a Venn diagram.

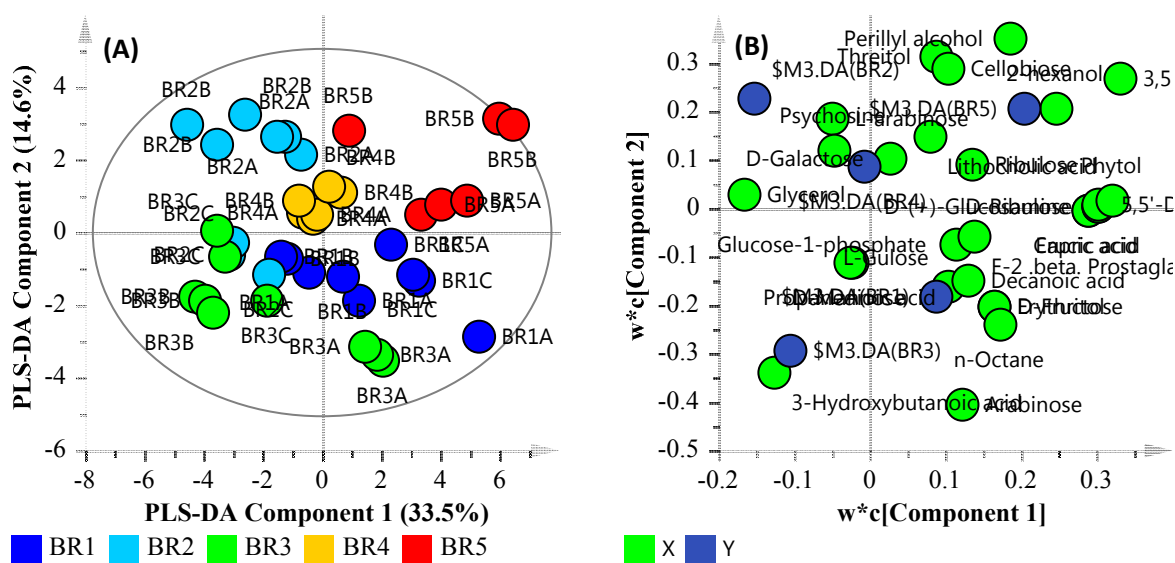


Figure 4. PLS-DA plot of the identified metabolites. (A) PLS-DA Score Scatter plot; (B) PLS-DA Loading Scatter plot.

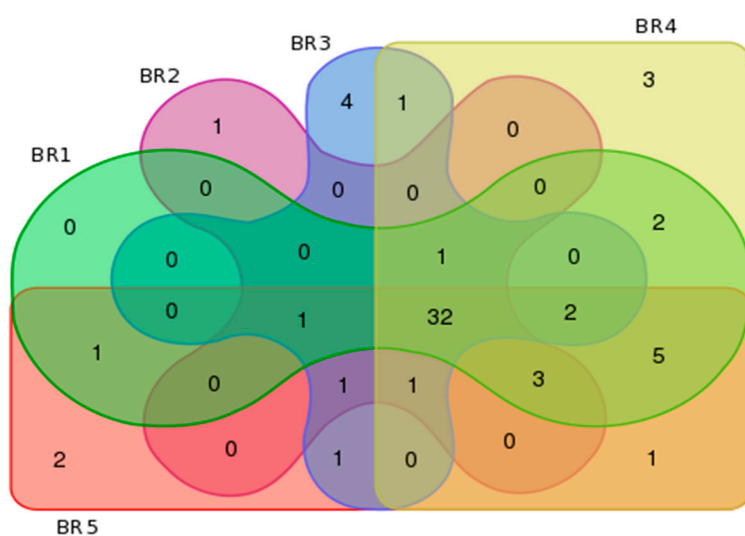


Figure 5. Metabolite similarity and uniqueness characterization.

Table 6. Most significant metabolites from the sampled river sites identified by based on their fold change (FC), *p*-value and Adjusted (Adj.) *p*-values.

Compound	Description	Fold Change	<i>p</i> -Value	Adj. <i>p</i> -Value
L-Gulose (5TMS)	Monosaccharide sugar	2.885793773	3.60×10^{-6}	5.00×10^{-2}
L-Arabinose (4TMS)	Sugar	1.995251285	0.20237	3.82×10^{-2}
Glycerol (3TMS)	Component of triglycerides and of phospholipids	1.850174576	0.41024	3.13×10^{-2}
α -D-Glucose-1-phosphate, dipotassium salt dihydrate		1.792927932	0.85638	9.72×10^{-3}
Psychosine sulfate (dTMS)	Lipid and intermediate in the biosynthesis of cerebroside	1.744904803	0.049444	4.58×10^{-2}
D-Cellobiose (1MEOX, 8TMS)	Disaccharide sugar	1.626482976	0.0061321	4.86×10^{-2}
2-methyl-2-butenedioic acid (2TMS)	Carboxylic acid	1.535874614	0.4597	2.71×10^{-2}
Prostaglandin F2 β (1MEOX, 4TMS)	Arachidonic acid metabolites	1.196188199	0.1738	3.96×10^{-2}
D-Threitol (4TMS)	End product of D-xylose metabolism	1.092677384	0.60615	1.74×10^{-2}
D-Fructose (5TMS)	Monosaccharide sugar	1.041734383	0.4944	2.08×10^{-2}
n-Octane	Component of Fatty acid metabolism	0.981496334	0.92237	3.47×10^{-3}
Perillyl alcohol (dTMS)	Isolated from the essential oils	0.959935677	0.60615	1.67×10^{-2}
Decanoic acid methyl ester (1TMS)	Constituent of many plants	0.956956828	0.44286	2.85×10^{-2}
D-Arabinose (4TMS)	Intermediate in biosynthesis of lipopolysaccharide	0.893785022	0.41024	3.06×10^{-2}
L-Tyrosine (3TMS)	Amino acid	0.834176724	0.87829	6.94×10^{-3}
Erucic acid methyl ester (1TMS)	Fatty acids	0.790950415	0.11213	4.17×10^{-2}
Capric acid (1TMS)	Fatty acids	0.790934596	0.11213	4.24×10^{-2}
D-Glucose 6-phosphate (1MEOX, 6TMS)	Aminosaccharide	0.782548013	0.07339	4.44×10^{-2}
Phytol (1TMS)	Constituent of chlorophyll	0.706423756	0.034756	4.65×10^{-2}
Unknown Compound 10 (MW = 206.2)		0.662675401	0.2944	3.47×10^{-2}
Erythritol (4TMS)	Sugar alcohol	0.659587922	0.24544	3.75×10^{-2}
3,6-anhydro-D-Galactose (dTMS)		0.6094551	0.088429	4.38×10^{-2}
D-Ribulose (1MEOX, 4TMS)	Monosaccharide sugar	0.317429352	0.014781	4.72×10^{-2}
D-Mannose (dTMS)	Carbohydrate	0.27712129	0.58678	1.81×10^{-2}
Lithocholic acid (2TMS)	Bile acid formed from chenodeoxycholate by bacterial action	0.203416434	0.58678	1.88×10^{-2}
Butanoic acid methyl ester (1TMS)	Fatty acid methyl ester	0.153370303	0.96669	2.78×10^{-3}
2-methylpropanedioic acid (2TMS)	Malonic acid derivative	0.152544336	0.34935	3.33×10^{-2}

3.6. Multi-Omics

As illustrated in the summary table (Table 7), an assessment of the water quality parameters in isolation is often difficult and tedious to decipher in terms of the system’s health and resilience; not to mention looking at the metagenomics and metabolomics data in isolation, due to the volume of data. An elevated result or a breach of the guidelines may not necessarily mean that the site or system is degraded. For example, the microbial indicators of the sites sampled suggest that sites BR₃, BR₄, and BR₅ may pose a risk to human health (and were indeed classed as low quality). However, as illustrated in the study by Ahmed et al. [52] of the same samples, only site BR₃ was observed to have a human wastewater signature. Likewise, sites BR₄ and BR₅ had elevated salinity levels according to the guidelines but it was noted that these sites were heavily influenced by the tide. As such, it is important to note that such data only provide a snapshot of the system at the time of sampling and may not represent the characteristics of the overall system at all times. One approach to overcome such problems is to sample the system more frequently (both temporarily and longitudinally). However, this will significantly increase the cost of analysis. An alternative approach that requires fewer samples to be collected is a multi-omics approach. Environmental multi-omics relies on a deeper analysis of the system being sampled in terms of bacterial diversity and metabolic output. Furthermore, it combines metadata to investigate relationships between sites. While it is ideal to do such an analysis over a period of time in order to establish seasonal trends, the study presented herein demonstrates its application and illustrates the added value of such an approach.

Table 7. Physico-chemical and microbial water quality summary.

BR Site	Monitoring Indicators												MAC *	
	Physico-Chemical									Microbial				
	Salinity	Turbidity	pH	Chlorophyll a	TP	FRP	TN	NO _x	NH ₄ ⁺	Metals	<i>E. coli</i>	<i>Enterococcus</i> spp.		FIB (combined)
BR ₁	N	N	N	Y	Y	Y	N	N	N	N	L	L	N	A
BR ₂	N	N	N	N	Y	Y	Y	Y	N	N	L	L	N	A
BR ₃	N	Y	N	N	Y	Y	Y	Y	N	N	H	H	Y	D
BR ₄	Y	Y	N	N	Y	Y	N	Y	N	N	H	H	Y	D
BR ₅	Y	Y	N	N	Y	Y	N	Y	N	N	H	H	Y	D

Note: * MAC is defined as the Microbial Water Quality Assessment Category.

As such, in order to assess the entire system (from site BR₁ through to BR₅ from the perspective of heavy metals, physical and chemical parameters, metabolites and bacterial diversity), first the multiple datasets collected need to be collated and analyzed using a multi-omics approach in order to see if the data provide insight into the river system’s health. Investigating complex systems in isolation, whether it be analyzing measurements or sites in isolation, without consideration of upstream and downstream conditions, can result in an incorrect assessment of overall health or degradation. To this end, a series of PLS-DA plots were created in order to combine the multiple datasets presented herein. Each dataset was first matched by site name and log transformed in SIMCA to normalize the data. This enabled the data to be interrogated and provided a greater depth of analysis compared to investigating each site and parameter in isolation. The following section details such an assessment using the MAC characterization (i.e., Class A and D; which is also the same grouping as turbidity), the salinity data (i.e., high and low salinity) and MAC classification in combination with low salinity site data to categorize sites for comparison.

3.6.1. Microbial Water Quality Assessment Category Class Assessment

After the data were uploaded into SIMCA individually, matched by sample location identifiers and log transformed, they were then grouped based on the MAC category of 'Class A' and 'Class D'. The resulting PLS-DA model was assessed by the linearity (R^2X and R^2Y) and predictability (Q^2), which were observed at 0.584, 0.987 and 0.750, respectively. This is indicative of a model that reasonably fits the data and has a good predictive capability (>0.7). Figure 6A illustrates the PLS-DA score scatter plot of the combined datasets grouped based on MAC values (i.e., Class A and Class D), and Figure 6B illustrates the loading scatter plot of the observed parameters.

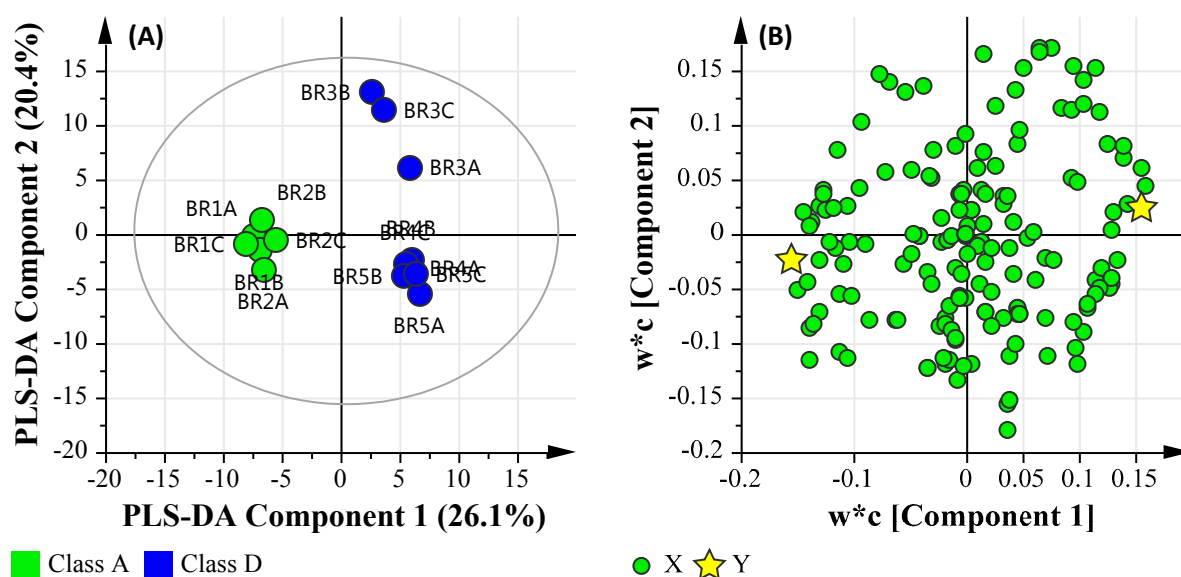


Figure 6. PLS-DA plot of the metadata and multi-omics datasets based the Microbial Water Quality Assessment Category class assessment. (A) PLS-DA Score Scatter plot; (B) PLS-DA Loading Scatter plot.

Using the MAC Class PLS-DA model, the dominant significant taxa classified at the class level for the 'Class A' pooled samples were *Acidobacteria*, *Alphaproteobacteria*, *Anaerolineae*, *Bacilli*, *Betaproteobacteria*, *Chlamydiae*, *Chloroflexi*, *Elusimicrobia*, *Fusobacteria*, *Gammaproteobacteria*, *Gemmatimonadetes*, *Holophagae*, *Ignavibacteria*, *Ktedonobacteria*, *Mollicutes*, *Negativicutes*, *Nitrospira*, *Opitutae*, *Spartobacteria*, *Spirochaetes*, *Thermodesulfobacteria*, *Verrucomicrobiae*, and *Zetaproteobacteria*. The dominant significant metabolic features were metabolites relating to carbohydrate metabolism (L-gulose, L-arabinose), glucagon signaling pathway (α -D-Glucose-1-phosphate, dipotassium salt dihydrate), and starch and sucrose metabolism (D-Cellobiose). Furthermore, no trace metals were correlated with the pool 'Class A' sample cohort.

In contrast, the dominant significant taxa classified at the class level for the 'Class D' pooled samples were *Armatimonadetes*, *Chlorobia*, *Chloroplast*, *Chrysiogenetes*, *Chthonomonadetes*, *Clostridia*, *Cyanobacteria*, *Deferribacteres*, *Dehalococcoidetes*, *Deinococci*, *Epsilonproteobacteria*, *Fibrobacteria*, *Flavobacteria*, *Lentisphaeria*, *Planctomycetacia*, *Sphingobacteria*, *Synergistia*, *Thermolithobacteria*, *Thermomicrobia*, and *Thermotogae*. The dominant significant metabolic features were metabolites relating to secondary bile acid biosynthesis (Lithocholic acid), carbohydrate metabolism (3,6-anhydro-D-galactose), fatty acid biosynthesis (capric acid), fructose and mannose metabolism (D-mannose), biosynthesis of unsaturated fatty acids (erucic acid methyl ester), and pentose and glucuronate interconversions (D-ribulose), in addition to chemical markers commonly found in human waste stream such as phytol mixture of isomers (manufacture of synthetic forms of vitamin E and vitamin K1), and osteoarthritis medication (D-glucosamine hydrochloride). Lastly, the trace metals of Al, Cr, Fe, Co, Ni, Cu, Zn and Pb were associated with the pooled 'Class D' sample cohort.

This suggests that 'Class D' pooled samples are correlated based on a number of factors, primarily bacteria that are known to cause or influence algae blooms (such as *Cyanobacteria*), organisms that lack aerobic respiration (*Clostridia*, *Synergistia*) and a number of green sulfur and non-sulfur bacteria (*Chlorobia*, *Thermomicrobia*), which are exacerbated due to the presence of pollutants (such as the presence of human waste stream indicators and heavy metals). Furthermore, bacteria capable of dehalogenating polychlorinated aliphatic alkanes and alkenes (*Dehalococcoidetes*) and organisms highly resistant to environmental hazards (*Deinococci*) were more abundant in Class D pooled samples. The presence of such organisms suggest the organisms within the sites are resistant to pollutants. However, the presence of *Fibrobacteria* suggests that commensal bacteria and opportunistic pathogens may also be present. In contrast, 'Class A' pooled samples were found to have organisms more commonly found in soil and aquatic environments, with no significant human waste-derived contaminants or metals present.

3.6.2. Salinity Assessment

The data were grouped based on salinity data which was classed as 'Low' (<1.0 ppt) and 'High' (~30 ppt). The resulting PLS-DA model was assessed by the linearity (R^2X and R^2Y) and predictability (Q^2), which were observed at 0.450, 0.983 and 0.911, respectively. This is indicative of a model that reasonably fits the data and has an excellent predictive capability (>0.9). Figure 7A illustrates the PLS-DA score scatter plot of the combined datasets grouped based on Salinity values (Low and High), and Figure 7B illustrates the loading scatter plot of the observed parameters.

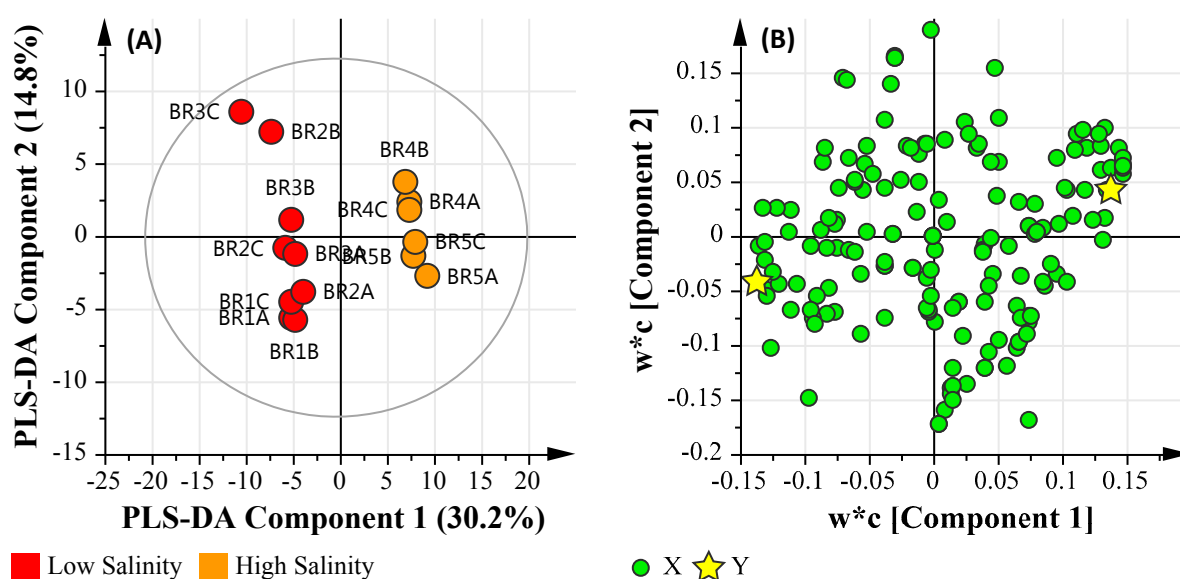


Figure 7. PLS-DA plot of the metadata and multi-omics datasets based the Microbial Water Quality Assessment Category class assessment. (A) PLS-DA Score Scatter plot; (B) PLS-DA Loading Scatter plot.

Using the salinity class PLS-DA model, the dominant significant taxa classified at the class level for the 'Low' salinity sample sites were: *Acidobacteria*, *Alphaproteobacteria*, *Anaerolineae*, *Bacilli*, *Betaproteobacteria*, *Chlamydiae*, *Chloroflexi*, *Elusimicrobia*, *Fusobacteria*, *Gammaproteobacteria*, *Gemmatimonadetes*, *Holophagae*, *Ignavibacteria*, *Ktedonobacteria*, *Negativicutes*, *Nitrospira*, *Opiritae*, *Spartobacteria*, *Spirochaetes*, *Thermodesulfobacteria*, *Verrucomicrobiae*, and *Zetaproteobacteria*. The dominant significant metabolic features were metabolites relating to carbohydrate metabolism (L-gulose, butanoic acid), alanine metabolism (propanedioic acid), Biosynthesis of secondary metabolites (glycerol). Furthermore, Al, Cr, Zn and Pb were correlated with the 'low' salinity pooled cohort.

In contrast, the dominant significant taxa classified at the class level for the ‘High’ salinity sample sites were: *Armatimonadetes*, *Caldilineae*, *Chlorobia*, *Chloroplast*, *Chrysiogenetes*, *Chthonomonadetes*, *Clostridia*, *Cyanobacteria*, *Deferribacteres*, *Deinococci*, *Epsilonproteobacteria*, *Fibrobacteria*, *Flavobacteria*, *Planctomycetacia*, *Sphingobacteria*, *Synergistia*, *Thermolithobacteria*, *Thermomicrobia*, and *Thermotogae*. The dominant significant metabolic features were metabolites relating to secondary bile acid biosynthesis (lithocholic acid), carbohydrate metabolism (3,6-anhydro-D-galactose), fatty acid biosynthesis (capric acid), fructose and mannose metabolism (D-mannose), biosynthesis of unsaturated fatty acids (erucic acid methyl ester), osteoarthritis medication (D-glucosamine hydrochloride), and pentose and glucuronate interconversions (D-ribulose). In addition to chemical markers commonly found in human waste streams, such as Phytol, and perillyl alcohol (a monoterpene isolated from the essential oils of lavandin, peppermint, spearmint, cherries, celery seeds, and several other plants) were also detected. Lastly, Fe was associated with the pooled high salinity sample cohort. Like the previous assessment, the addition of salinity as a grouping highlights the presence of photosynthetic bacteria in addition to bacteria that are resilient to pollution sources.

3.6.3. Microbial Water Quality Assessment Category Class A and Low Salinity Assessment

As illustrated in Figure 6, sites BR₁ and BR₂ were grouped apart from BR₃. In order to further analyze this sub-grouping, the ‘High’ salinity based sites (BR₄ and BR₅) were removed and a subsequent PLS-DA comparison was undertaken. Figure 8 illustrates the PLS-DA comparison based on Microbial Water Quality Assessment Category class and ‘Low’ salinity. The resulting PLS-DA model was assessed by the linearity (R^2X and R^2Y) and predictability (Q^2), which were observed at 0.560, 0.964 and 0.657, respectively. This is indicative of a model that reasonably fits the data and has an average predictive capability (≥ 0.5).

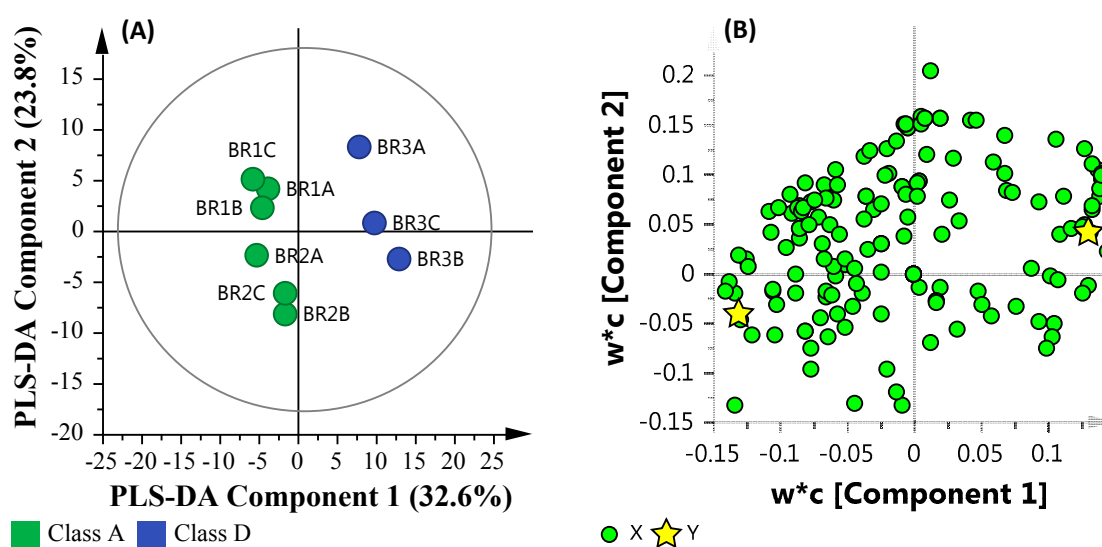


Figure 8. PLS-DA plot of the metadata and multi-omics datasets based the Microbial Water Quality Assessment Category class and low salinity assessment. (A) PLS-DA Score Scatter plot; (B) PLS-DA Loading Scatter plot.

This comparison highlights the increased presence of metals, short-chain fatty acids (SCFA) and sugars in site BR₃ when compared with sites BR₁ and BR₂. Furthermore, the increased abundance of bacteria belonging to *Acidobacteria*, *Actinobacteria*, *Armatimonadetes*, *Chloroflexi*, *Chloroplast*, *Chrysiogenetes*, *Chthonomonadetes*, *Dehalococcoidetes*, *Fibrobacteria*, *Sphingobacteria*, and *Thermolithobacteria* suggests an environment that is capable of dehalogenating polychlorinated aliphatic alkanes and alkenes (*Dehalococcoidetes*) and the presence of *Fibrobacteria* suggests that commensal bacteria and opportunistic pathogens may also be present.

4. Discussion

Bacterial populations were observed to be affected by the nature of the sites sampled. BR₁ site was observed to be rich in soil- and water-based bacteria, *Ralstonia* and *Bordetella* from *Burkholderiaceae* family, mostly of wildlife/domestic animal sources and plant origin. Also, expectedly, a large number of *Actinomyces* were also observed at BR₁ and BR₂ sites. The *Burkholderiaceae* population dropped at the agriculturally prominent site, BR₂. Greater values for parameters such as temperature, pH, phosphates and nitrogen compounds resulted in a greater abundance of photosynthetic populations such as *Cyanobacteria* and other chloroplast-containing bacteria. The presence of cyanobacterial family II is possibly indicative of increased occurrence of sulphur compounds at BR₂. It was observed that the populations of *Alteromonas* and related families within the *Alteromonadales* increased at BR₂. This was unexpected as these bacteria are generally found in marine environments. However, it is probable that the tidal nature of the Brisbane River (86 km from the mouth) combined with high dissolved oxygen content [53] (9.3 mg·L⁻¹) and added phosphorous salts (320 µg·L⁻¹) might have resulted in higher *Alteromonas*, possibly due to the high phosphate metabolizing ability of organophosphorus acid anhydrolase (OPAA) (EC3.1.8.2) expression systems [54]. Due to the vicinity around wastewater treatment plants and other similar activities, site BR₃ was expected to have greater abundances of *Actinomyces*, *Streptomyces*, and *Frankia* and other related facultative anaerobic bacteria. The site was observed to have considerably greater turbidity with respect to previously reported values of about 50–60 NTU [53]. *Actinomyces* are known to decay organic matter, especially in nutrient-rich environments such as wetlands [55] and various river samples [56], especially in association with *Sphingobacteria* around areas of human and animal activities. The co-occurrence of *Actinomyces* with *Sphingobacteria* was expected as it has been reported that the latter are efficient degraders of geosmin and 2-methylisoborneol, the compounds produced by *Actinomyces*. These compounds have been reported to be responsible for increasing turbidity and odor of the riverine water system [57]. The current findings are therefore in line with previous reports, as greater turbidity was observed at site BR₃ relative to sites BR₁ and, especially, BR₂. Similarly, greater turbidity at downstream sites of BR₄ and BR₅ may be partially attributed to less abundant sphingobacterial populations at those sites. It is also important to note that fecal coliforms, which comprises such organisms as *Escherichia coli*, *Klebsiella pneumoniae* and *Enterobacter aerogenes* (order *Enterobacteriales*) and faecal streptococci such as *Enterococcus* (order *Lactobacillales*) were not observed in significant numbers, although the study by Ahmed et al. [33] detected the presence of human and non-human fecal molecular markers.

The sites BR₄ and BR₅ are located very close to BR mouth, at the distances of about 22 km and 13 km, respectively. The area is considered as an inter-tidal zone, with a decreased flow-rate. The inter-tidal nature was associated with decreased levels of turbidity (15.3 NTU at BR₄ with respect to 137.3 NTU at BR₃) and dissolved oxygen. Due to the contribution of downstream oceanic and upstream sedimentation salts (from silts, soils, human and animal activities), inter-tidal zones, especially tidal flats have reportedly higher amounts of salinity. The higher content of deposited clay in this region also contributes towards increased salinity as compared to low clay soils or sands [58]. The high nutrient deposition combined with low flow rate and slightly anoxic nature of water at site BR₄ and BR₅ sites possibly resulted in increased populations of *Rhodobacteria* and *Rhodospiralles* such as *Rhodobacter*, *Acetobacter*, and *Azospirillum* spp. among others. Most of these bacteria are known to be chemo- and photo-autotrophic in nature and reportedly occur around Mangrove ecosystems (which are common around Brisbane). A significant decrease in nitrogen content at site BR₄ and BR₅ could be attributed to the nitrogen fixing and phosphate solubilisation abilities of these bacteria [59]. Other bacterial classes with a population increase were from Gamma-proteobacteria, with the order *Incertae sedis* members concentrated at site BR₄ and *Pseudomonadales* (4%) at site BR₅. It is very likely that the significant decrease in phosphates, nitrogen and turbidity was caused by the solubilization facilitated by *Pseudomonas* and related species at site BR₅ [59].

It was noticed that the lower abundances of *Burkholderiales* at sites BR₂ and BR₃ were associated with decreased levels of sugars and sugar alcohols. Similarly, the greater abundances in *Cyanobacteria*

at BR₂ and *Actinomycetes* at BR₃ are likely to influence the observed greater concentrations of SCFAs, such as butanoic and propanedioic acid. Such SCFAs enhance the biofilm formation ability of bacteria. In particular, exposure to lower concentrations of SCFAs, such as ca. 6 mM, enhances the biofilm formation ability of *Actinomycetes* bacteria [60]. Similarly, an increased level of erythritol could also be linked to bacterial biofilm formation. Although the contribution of erythritol to biofilm formation was observed to be less than SFCA, its greater concentration across all the sites may compensate for the deficit. Furthermore, it has been shown that erythritol, along with amino acids such as asparagine and phenylalanine, act as major contributory metabolites towards biofilm formation [61]. The abundance of SCFAs may also be indicative of mixotroph organisms able to utilize different SCFAs as organic carbon sources, either during growth or nutrient stress lipogenic phases [62]. Lastly, the sugar levels increased again at sites BR₄ and BR₅, very likely due to the increased fermentation caused by *Rhodobacteria*, *Rhodospirilli*, Gamma-proteobacteria and, especially, photosynthetic bacteria. As such, based on the metabolites observed, sites BR₂ and BR₃ have metabolites present that suggest a system that has potential to form biofilms and/or a community of mixotrophs that utilize SCFAs and that sites BR₄ and BR₅ are environments undergoing degradation.

5. Conclusions

Multiple characterizations of the BR system were performed by various genomic, ionic and metabolic methods. The metagenomics output indicated a presence of high levels of freshwater bacteria such as *Burkholdariales* and lower levels of *Actinomycetes* and *Rhodospirillae* in the upstream sites. In contrast, the population levels reversed in downstream sites, affected by salinity, pH and oxygen availability changes. Human interference was indicated by the increasing populations of *Actinomycetes* (BR₃), including fecal bacteria and *Pseudomonadales* (BR₄ and BR₅). Greater abundances of these populations in downstream areas was also possibly caused by the increased levels of sugar alcohols, such as erythritol, SCFAs and aromatic amino acids, contributing heavily towards biofilm production. Overall, the multi-omics approach presented herein was able to provide a deeper insight into water quality contamination and riverine health in terms of metabolic and microbial properties that are not possible using traditional water quality methods. As such, a multi-omics based approach should be considered when characterizing complex environmental systems, in particular when assessing the impacts of agricultural practices, sewage treatment and environmental endpoints.

Acknowledgments: The authors would like to acknowledge the assistance and support provided by the CSIRO's Microbiology Water Quality Sciences Group, in particular the support of J. Sidhu and A. Palmer for their assistance in collecting water samples used in this study. The authors would also like to thank and acknowledge the financial support of the CSIRO Land and Water business unit. Amplicon sequence data were processed and analyzed using the resources of the Minnesota Supercomputing Institute.

Author Contributions: D.J.B. conceived, designed, and performed the metabolomics experiments, metals, statistical analysis and wrote the paper. A.V.K. assisted with the metabolomics experiments and in interpreting the metabolomics data. W.A. conceived, designed, and performed the metagenomics experiments. S.C. assisted with collating and analyzing the complimentary EHMP and metadata. P.D.M. performed the ICP-MS analysis and assisted in the interpretation of data. C.S. processed and analyzed amplicon sequencing data and provided review of the manuscript. M.J.S. provided review of the manuscript. E.A.P. assisted in interpreting the data and preparing the manuscript.

Conflicts of Interest: The authors declare no conflict of interest.

References

1. Abram, F. Systems-based approaches to unravel multi-species microbial community functioning. *Comput. Struct. Biotechnol. J.* **2015**, *13*, 24–32. [[CrossRef](#)] [[PubMed](#)]
2. Robinson, A.M.; Gondalia, S.V.; Karpe, A.V.; Eri, R.; Beale, D.J.; Morrison, P.D.; Palombo, E.A.; Nurgali, K. Fecal microbiota and metabolome in a mouse model of spontaneous chronic colitis: Relevance to human inflammatory bowel disease. *Inflamm. Bowel Dis.* **2016**, *22*, 2767–2787. [[CrossRef](#)] [[PubMed](#)]

3. Kumarasingha, R.; Karpe, A.V.; Preston, S.; Yeo, T.C.; Lim, D.S.L.; Tu, C.L.; Luu, J.; Simpson, K.J.; Shaw, J.M.; Gasser, R.B.; et al. Metabolic profiling and in vitro assessment of anthelmintic fractions of *Picria fel-terrae* Lour. *Int. J. Parasitol.* **2016**, *6*, 171–178. [[CrossRef](#)] [[PubMed](#)]
4. Bundy, J.G.; Davey, M.P.; Viant, M.R. Environmental metabolomics: A critical review and future perspectives. *Metabolomics* **2009**, *5*, 3–21. [[CrossRef](#)]
5. Hultman, J.; Waldrop, M.P.; Mackelprang, R.; David, M.M.; McFarland, J.; Blazewicz, S.J.; Harden, J.; Turetsky, M.R.; McGuire, A.D.; Shah, M.B.; et al. Multi-omics of permafrost, active layer and thermokarst bog soil microbiomes. *Nature* **2015**, *521*, 208–212. [[CrossRef](#)] [[PubMed](#)]
6. Jones, O.A.H.; Sdepanian, S.; Lofts, S.; Svendsen, C.; Spurgeon, D.J.; Maguire, M.L.; Griffin, J.L. Metabolomic analysis of soil communities can be used for pollution assessment. *Environ. Toxicol. Chem.* **2014**, *33*, 61–64. [[CrossRef](#)] [[PubMed](#)]
7. Desai, C.; Pathak, H.; Madamwar, D. Advances in molecular and “-omics” technologies to gauge microbial communities and bioremediation at xenobiotic/anthropogen contaminated sites. *Bioresour. Technol.* **2010**, *101*, 1558–1569. [[CrossRef](#)] [[PubMed](#)]
8. Bullock, A.; Ziervogel, K.; Ghobrial, S.; Jalowska, A.; Arnosti, C. Microbial activities and organic matter degradation at three sites in the coastal North Atlantic: Variations in DOC turnover times and potential for export off the shelf. *Mar. Chem.* **2015**, *177*, 388–397. [[CrossRef](#)]
9. Date, Y.; Nakanishi, Y.; Fukuda, S.; Kato, T.; Tsuneda, S.; Ohno, H.; Kikuchi, J. New monitoring approach for metabolic dynamics in microbial ecosystems using stable-isotope-labeling technologies. *J. Biosci. Bioeng.* **2010**, *110*, 87–93. [[CrossRef](#)] [[PubMed](#)]
10. Hook, S.E.; Osborn, H.L.; Spadaro, D.A.; Simpson, S.L. Assessing mechanisms of toxicant response in the amphipod *Melita plumulosa* through transcriptomic profiling. *Aquat. Toxicol.* **2014**, *146*, 247–257. [[CrossRef](#)] [[PubMed](#)]
11. Osborn, H.L.; Hook, S.E. Using transcriptomic profiles in the diatom *Phaeodactylum tricornutum* to identify and prioritize stressors. *Aquat. Toxicol.* **2013**, *138–139*, 12–25. [[CrossRef](#)] [[PubMed](#)]
12. Llewellyn, C.A.; Sommer, U.; Dupont, C.L.; Allen, A.E.; Viant, M.R. Using community metabolomics as a new approach to discriminate marine microbial particulate organic matter in the western English Channel. *Prog. Oceanogr.* **2015**, *137*, 421–433. [[CrossRef](#)]
13. Griffiths, W.J. *Metabolomics, Metabonomics and Metabolite Profiling*; Royal Society of Chemistry: Cambridge, UK, 2008.
14. Harrigan, G.G.; Goodacre, R. *Metabolic Profiling: Its Role in Biomarker Discovery and Gene Function Analysis*; Springer Science & Business Media: New York, NY, USA, 2012.
15. Lindon, J.C.; Holmes, E.; Nicholson, J.K. *Metabonomics Techniques and Applications to Pharmaceutical Research & Development*. *Pharm. Res.* **2006**, *23*, 1075–1088. [[PubMed](#)]
16. Gómez-Canela, C.; Miller, T.H.; Bury, N.R.; Tauler, R.; Barron, L.P. Targeted metabolomics of *Gammarus pulex* following controlled exposures to selected pharmaceuticals in water. *Sci. Total Environ.* **2016**, *562*, 777–788. [[CrossRef](#)] [[PubMed](#)]
17. Cao, C.; Wang, W.-X. Bioaccumulation and metabolomics responses in oysters *Crassostrea hongkongensis* impacted by different levels of metal pollution. *Environ. Pollut.* **2016**, *216*, 156–165. [[CrossRef](#)] [[PubMed](#)]
18. Ji, C.; Yu, D.; Wang, Q.; Li, F.; Zhao, J.; Wu, H. Impact of metal pollution on shrimp *Crangon affinis* by NMR-based metabolomics. *Mar. Pollut. Bull.* **2016**, *106*, 372–376. [[CrossRef](#)] [[PubMed](#)]
19. Thakur, N.L.; Jain, R.; Natalio, F.; Hamer, B.; Thakur, A.N.; Müller, W.E.G. Marine molecular biology: An emerging field of biological sciences. *Biotechnol. Adv.* **2008**, *26*, 233–245. [[CrossRef](#)] [[PubMed](#)]
20. Kimes, N.E.; Callaghan, A.V.; Aktas, D.F.; Smith, W.L.; Sunner, J.; Golding, B.; Drozdowska, M.; Hazen, T.C.; Sufliata, J.M.; Morris, P.J. Metagenomic analysis and metabolite profiling of deep-sea sediments from the Gulf of Mexico following the Deepwater Horizon oil spill. *Front. Microbiol.* **2013**, *4*, 50. [[CrossRef](#)] [[PubMed](#)]
21. Yang, F.-C.; Chen, Y.-L.; Tang, S.-L.; Yu, C.-P.; Wang, P.-H.; Ismail, W.; Wang, C.-H.; Ding, J.-Y.; Yang, C.-Y.; et al. Integrated multi-omics analyses reveal the biochemical mechanisms and phylogenetic relevance of anaerobic androgen biodegradation in the environment. *ISME J.* **2016**, *10*, 1967–1983. [[CrossRef](#)] [[PubMed](#)]
22. Beale, D.J.; Karpe, A.V.; McLeod, J.D.; Gondalia, S.V.; Muster, T.H.; Othman, M.Z.; Palombo, E.A.; Joshi, D. An “omics” approach towards the characterisation of laboratory scale anaerobic digesters treating municipal sewage sludge. *Water Res.* **2016**, *88*, 346–357. [[CrossRef](#)] [[PubMed](#)]

23. McLeod, J.D.; Othman, M.Z.; Beale, D.J.; Joshi, D. The use of laboratory scale reactors to predict sensitivity to changes in operating conditions for full-scale anaerobic digestion treating municipal sewage sludge. *Bioresour. Technol.* **2015**, *189*, 384–390. [CrossRef] [PubMed]
24. Tan, B.; Ng, C.; Nshimiyimana, J.P.; Loh, L.L.; Gin, K.Y.H.; Thompson, J.R. Next-generation sequencing (NGS) for assessment of microbial water quality: Current progress, challenges, and future opportunities. *Front. Microbiol.* **2015**, *6*, 1027. [CrossRef] [PubMed]
25. Gomez-Alvarez, V.; Revetta, R.P.; Santo Domingo, J.W. Metagenomic Analyses of Drinking Water Receiving Different Disinfection Treatments. *Appl. Environ. Microbiol.* **2012**, *78*, 6095–6102. [CrossRef] [PubMed]
26. Van Rossum, T.; Peabody, M.A.; Uyaguari-Diaz, M.I.; Cronin, K.I.; Chan, M.; Slobodan, J.R.; Nesbitt, M.J.; Suttle, C.A.; Hsiao, W.W.L.; Tang, P.K.C.; et al. Year-long metagenomic study of river microbiomes across land use and water quality. *Front. Microbiol.* **2015**, *6*, 1405. [CrossRef] [PubMed]
27. Beale, D.J.; Barratt, R.; Marlow, D.R.; Dunn, M.S.; Palombo, E.A.; Morrison, P.D.; Key, C. Application of metabolomics to understanding biofilms in water distribution systems: A pilot study. *Biofouling* **2013**, *29*, 283–294. [CrossRef] [PubMed]
28. Davis, J.M.; Ekman, D.R.; Teng, Q.; Ankley, G.T.; Berninger, J.P.; Cavallin, J.E.; Jensen, K.M.; Kahl, M.D.; Schroeder, A.L.; Villeneuve, D.L.; et al. Linking field-based metabolomics and chemical analyses to prioritize contaminants of emerging concern in the Great Lakes basin. *Environ. Toxicol. Chem.* **2016**, *35*, 2493–2502. [CrossRef] [PubMed]
29. HealthyWaterways. 2012 Brisbane River Sitemap. Available online: <http://healthywaterways.org/resources/documents/2012-brisbane-river-sitemap-doc-3476> (accessed on 3 November 2016).
30. Oshiro, R.K. *Method 1603: Escherichia coli (E. coli) in Water by Membrane Filtration Using Modified Membrane Thermotolerant Escherichia coli Agar (Modified mTEC)*; United States Environmental Protection Agency: Washington, DC, USA, 2002.
31. Ahmed, W.; Stewart, J.; Powell, D.; Gardner, T. Evaluation of the host-specificity and prevalence of enterococci surface protein (esp) marker in sewage and its application for sourcing human fecal pollution. *J. Environ. Qual.* **2008**, *37*, 1583–1588. [CrossRef] [PubMed]
32. Ahmed, W.; Sawant, S.; Huygens, F.; Goonetilleke, A.; Gardner, T. Prevalence and occurrence of zoonotic bacterial pathogens in surface waters determined by quantitative PCR. *Water Res.* **2009**, *43*, 4918–4928. [CrossRef] [PubMed]
33. Ahmed, W.; Staley, C.; Sadowsky, M.J.; Gyawali, P.; Sidhu, J.P.S.; Palmer, A.; Beale, D.J.; Toze, S. Toolbox approaches using molecular markers and 16S rRNA gene amplicon data sets for identification of fecal pollution in surface water. *Appl. Environ. Microbiol.* **2015**, *81*, 7067–7077. [CrossRef] [PubMed]
34. Claesson, M.J.; Wang, Q.; O’Sullivan, O.; Greene-Diniz, R.; Cole, J.R.; Ross, R.P.; O’Toole, P.W. Comparison of two next-generation sequencing technologies for resolving highly complex microbiota composition using tandem variable 16S rRNA gene regions. *Nucleic Acids Res.* **2010**, *38*, e200. [CrossRef] [PubMed]
35. Youssef, N.; Sheik, C.S.; Krumholz, L.R.; Najjar, F.Z.; Roe, B.A.; Elshahed, M.S. Comparison of species richness estimates obtained using nearly complete fragments and simulated pyrosequencing-generated fragments in 16S rRNA gene-based environmental surveys. *Appl. Environ. Microbiol.* **2009**, *75*, 5227–5236. [CrossRef] [PubMed]
36. Schloss, P.D.; Westcott, S.L.; Ryabin, T.; Hall, J.R.; Hartmann, M.; Hollister, E.B.; Lesniewski, R.A.; Oakley, B.B.; Parks, D.H.; Robinson, C.J. Introducing mothur: Open-source, platform-independent, community-supported software for describing and comparing microbial communities. *Appl. Environ. Microbiol.* **2009**, *75*, 7537–7541. [CrossRef] [PubMed]
37. Aronesty, E. Comparison of sequencing utility programs. *Open Bioinform. J.* **2013**, *7*, 1–8. [CrossRef]
38. Pruesse, E.; Quast, C.; Knittel, K.; Fuchs, B.M.; Ludwig, W.; Peplies, J.; Glöckner, F.O. SILVA: A comprehensive online resource for quality checked and aligned ribosomal RNA sequence data compatible with ARB. *Nucleic Acids Res.* **2007**, *35*, 7188–7196. [CrossRef] [PubMed]
39. Huse, S.M.; Welch, D.M.; Morrison, H.G.; Sogin, M.L. Ironing out the wrinkles in the rare biosphere through improved OTU clustering. *Environ. Microbiol.* **2010**, *12*, 1889–1898. [CrossRef] [PubMed]
40. Kunin, V.; Engelbrektson, A.; Ochman, H.; Hugenholtz, P. Wrinkles in the rare biosphere: Pyrosequencing errors can lead to artificial inflation of diversity estimates. *Environ. Microbiol.* **2010**, *12*, 118–123. [CrossRef] [PubMed]

41. Edgar, R.C.; Haas, B.J.; Clemente, J.C.; Quince, C.; Knight, R. UCHIME improves sensitivity and speed of chimera detection. *Bioinformatics* **2011**, *27*, 2194–2200. [[CrossRef](#)] [[PubMed](#)]
42. Cole, J.R.; Wang, Q.; Cardenas, E.; Fish, J.; Chai, B.; Farris, R.J.; Kulam-Syed-Mohideen, A.; McGarrell, D.M.; Marsh, T.; Garrity, G.M. The Ribosomal Database Project: Improved alignments and new tools for rRNA analysis. *Nucleic Acids Res.* **2009**, *37*, D141–D145. [[CrossRef](#)] [[PubMed](#)]
43. Karpe, A.V.; Beale, D.J.; Godhani, N.B.; Morrison, P.D.; Harding, I.H.; Palombo, E.A. Untargeted metabolic profiling of winery-derived biomass waste degradation by *Penicillium chrysogenum*. *J. Agric. Food Chem.* **2015**, *63*, 10696–10704. [[CrossRef](#)] [[PubMed](#)]
44. Beale, D.; Morrison, P.; Key, C.; Palombo, E. Metabolic profiling of biofilm bacteria known to cause microbial influenced corrosion. *Water Sci. Technol.* **2014**, *69*, 1–8. [[CrossRef](#)] [[PubMed](#)]
45. Beale, D.J.; Marney, D.; Marlow, D.R.; Morrison, P.D.; Dunn, M.S.; Key, C.; Palombo, E.A. Metabolomic analysis of *Cryptosporidium parvum* oocysts in water: A proof of concept demonstration. *Environ. Pollut.* **2013**, *174*, 201–203. [[CrossRef](#)] [[PubMed](#)]
46. Karpe, A.V.; Beale, D.J.; Morrison, P.D.; Harding, I.H.; Palombo, E.A. Untargeted metabolic profiling of vitis vinifera during Fungal Degradation. *FEMS Microbiol. Lett.* **2015**. [[CrossRef](#)] [[PubMed](#)]
47. Karpe, A.; Beale, D.; Godhani, N.; Morrison, P.; Harding, I.; Palombo, E. Untargeted metabolic profiling of winery-derived biomass waste degradation by *Aspergillus niger*. *J. Chem. Technol. Biotechnol.* **2015**, *197*, 1–12.
48. Fiehn, O.; Robertson, D.; Griffin, J.; van der Werf, M.; Nikolau, B.; Morrison, N.; Sumner, L.W.; Goodacre, R.; Hardy, N.W.; Taylor, C. The metabolomics standards initiative (MSI). *Metabolomics* **2007**, *3*, 175–178. [[CrossRef](#)]
49. Australian Water Association (AWA). *Australian and New Zealand Guidelines for Fresh and Marine Water Quality. Volume 1, The Guidelines*; Australian and New Zealand Environment and Conservation Council, Agriculture and Resource Management Council of Australia and New Zealand: Artarmon, Sydney, Australia, 2000.
50. Ahmed, W.; Sidhu, J.P.S.; Toze, S. Evaluation of the nifH gene marker of methanobrevibacter smithii for the detection of sewage pollution in environmental waters in southeast Queensland, Australia. *Environ. Sci. Technol.* **2012**, *46*, 543–550. [[CrossRef](#)] [[PubMed](#)]
51. Ahmed, W.; Powell, D.; Goonetilleke, A.; Gardner, T. Detection and source identification of faecal pollution in non-sewered catchment by means of host-specific molecular markers. *Water Sci. Technol.* **2008**, *58*, 579–586. [[CrossRef](#)] [[PubMed](#)]
52. Ahmed, W.; Sidhu, J.P.S.; Smith, K.; Beale, D.J.; Gyawali, P.; Tozea, S. Distributions of fecal markers in wastewater from different climatic zones for human fecal pollution tracking in Australian surface waters. *Appl. Environ. Microbiol.* **2016**, *82*, 1316–1323. [[CrossRef](#)] [[PubMed](#)]
53. EHMP, Ecosystem Health Monitoring Program 2005–2006 Annual Technical Report. Available online: http://www.ehmp.org/media/scripts/doc_download.aspx?did=721 (accessed on 15 June 2007).
54. Cheng, T.-C.; DeFrank, J.J.; Rastogi, V.K. *Alteromonas* prolidase for organophosphorus G-agent decontamination. *Chem. Biol. Interact.* **1999**, *119–120*, 455–462. [[CrossRef](#)]
55. Huang, L.; Gao, X.; Liu, M.; Du, G.; Guo, J.; Ntakirutimana, T. Correlation among soil microorganisms, soil enzyme activities, and removal rates of pollutants in three constructed wetlands purifying micro-polluted river water. *Ecol. Eng.* **2012**, *46*, 98–106. [[CrossRef](#)]
56. Jeong, J.-Y.; Park, H.-D.; Lee, K.-H.; Weon, H.-Y.; Ka, J.-O. Microbial community analysis and identification of alternative host-specific fecal indicators in fecal and river water samples using pyrosequencing. *J. Microbiol.* **2011**, *49*, 585. [[CrossRef](#)] [[PubMed](#)]
57. Xue, Q.; Shimizu, K.; Sakharkar, M.K.; Utsumi, M.; Cao, G.; Li, M.; Zhang, Z.; Sugiura, N. Geosmin degradation by seasonal biofilm from a biological treatment facility. *Environ. Sci. Pollut. Res.* **2012**, *19*, 700–707. [[CrossRef](#)] [[PubMed](#)]
58. Yu, J.; Li, Y.; Han, G.; Zhou, D.; Fu, Y.; Guan, B.; Wang, G.; Ning, K.; Wu, H.; Wang, J. The spatial distribution characteristics of soil salinity in coastal zone of the Yellow River Delta. *Environ. Earth Sci.* **2014**, *72*, 589–599. [[CrossRef](#)]
59. Shakilabanu, S. Biodiversity of plant growth promoting rhizobacteria in mangrove ecosystem—A review. *Int. J. Pharm. Biol. Arch.* **2012**, *3*, 3.
60. Yoneda, S.; Kawarai, T.; Narisawa, N.; Tuna, E.B.; Sato, N.; Tsugane, T.; Saeki, Y.; Ochiai, K.; Senpuku, H. Effects of short-chain fatty acids on *Actinomyces naeslundii* biofilm formation. *Mol. Oral Microbiol.* **2013**, *28*, 354–365. [[CrossRef](#)] [[PubMed](#)]

61. Ylla, I.; Canhoto, C.; Romani, A.M. Effects of Warming on Stream Biofilm Organic Matter Use Capabilities. *Microb. Ecol.* **2014**, *68*, 132–145. [[CrossRef](#)] [[PubMed](#)]
62. Chandra, R.; Arora, S.; Rohit, M.V.; Venkata Mohan, S. Lipid metabolism in response to individual short chain fatty acids during mixotrophic mode of microalgal cultivation: Influence on biodiesel saturation and protein profile. *Bioresour. Technol.* **2015**, *188*, 169–176. [[CrossRef](#)] [[PubMed](#)]



© 2017 by the authors. Licensee MDPI, Basel, Switzerland. This article is an open access article distributed under the terms and conditions of the Creative Commons Attribution (CC BY) license (<http://creativecommons.org/licenses/by/4.0/>).